

1 Disclaimer: This is a pre-publication version. Readers are recommended to consult the
2 full published version for accuracy and citation. Published in *Limnology and*
3 *Oceanography: Methods*, 13, 673–686 (2015), doi: 10.1002/lom3.10057.
4

5 **Combined uncertainty estimation for the determination of the dissolved iron**
6 **amount content in seawater using flow injection with chemiluminescence**
7 **detection.**

8
9 G. H. Floor^{1a}, R. Clough², M. C. Lohan², S. J. Ussher², P. J. Worsfold², C. R. Quétel^{1*}.

10 1. Institute for Reference Materials and Measurements, Joint Research Centre–European Commission,
11 111 Retieseweg, 2440 Geel, Belgium.

12 2. Biogeochemistry Research Centre, School of Geography, Earth and Environmental Sciences, Plymouth
13 University, Plymouth, PL4 8AA, United Kingdom

14 a: Currently at GFZ German Research Centre for Geosciences, Helmholtz Centre Potsdam,
15 Telegrafenberg, 14473 Potsdam, Germany

16 * Corresponding author: Christophe.Quetel@ec.europa.eu

17 **Acknowledgements**

18 This work was financially supported by the EMRP via JRP-ENV05 (Metrology for ocean salinity and acidity,
19 GF) and JRP-ENV05-REG1 (RC). The EMRP is jointly funded by the EMRP participating countries within
20 EURAMET and the European Union. ML was supported by a Natural Environment Research Council
21 (NERC) grant NE/H004475/1. SU was supported by a Marie Curie Career Integration Grant (PCIG-GA-
22 2012-333143 DISCOSAT) from the European Commission. GF acknowledges J. Snell and T. Linsinger for
23 fruitful discussions.
24

25 **Abstract**

26 This work assesses the components contributing to the combined uncertainty budget associated with the
27 measurement of the Fe amount content by flow injection chemiluminescence (FI-CL) in <0.2 µm filtered
28 and acidified seawater samples. Amounts of loaded standard solutions and samples were determined
29 gravimetrically by differential weighing. Up to 5% variations in the loaded masses were observed during
30 measurements, in contradiction to the usual assumptions made when operating under constant loading
31 time conditions. Hence signal intensities (V) were normalised to the loaded mass and plots of average
32 normalized intensities (in V kg⁻¹) versus values of the Fe amount content (in nmol kg⁻¹) added to a 'low
33 level' iron seawater matrix were used to produce the calibration graphs. The measurement procedure
34 implemented and the uncertainty estimation process developed were validated from the agreement
35 obtained with consensus values for three SAFe and GEOTRACES reference materials (D2, GS and GD).
36 Relative expanded uncertainties for peak height and peak area based results were estimated to be
37 around 12% and 10% (k=2) respectively. The most important contributory factors were the uncertainty
38 on the sensitivity coefficient (i.e. calibration slope) and within-sequence-stability (i.e. the signal stability
39 measured over several hours of operation; in this case 32 h). Therefore, an uncertainty estimation based
40 on the intensity repeatability alone, as is often done in FI-CL studies, is not a realistic estimation of the
41 overall uncertainty of the procedure.

42

43

44 **Introduction**

45 The ocean acts as both a sink and a source for carbon dioxide and plays an important role in regulating
46 the global climate system (Boyd and Elwood, 2010). The dynamics of the ocean and its interaction with
47 the atmosphere are strongly linked to the properties of seawater. Elements such as Fe limit marine
48 primary production in approximately one third of the world's oceans (Ussher et al., 2013) and thus may
49 have a profound effect on plankton communities and the global carbon cycle (Martin and Fitzwater, 1988;
50 Mills et al., 2004). More reliable determinations of micronutrient elements in marine waters are thus
51 essential to enhance our understanding of their impact on ocean productivity and processes (e.g. ocean
52 acidification). Therefore, robust and fully validated measurement procedures are necessary, accompanied
53 by an estimation of the overall uncertainty budget.

54 The international standard ISO/IEC 17025 (2005) states that the performance of a measurement
55 procedure should be evaluated based on one or a combination of the following approaches: a) the use of
56 reference materials, b) the comparison of results achieved with other methods, c) inter-laboratory
57 comparison, d) systematic assessments of the factors influencing the result and e) the assessment of the
58 uncertainty of the results. The Fe content of commercially available certified reference materials is at
59 least one order of magnitude higher than most open ocean waters and are thus of limited use for
60 method development. Therefore, test materials from inter-laboratory comparison exercises are often used
61 instead, e.g. those collected as part of the IRONAGES, SAFe and GEOTRACES studies. However, Bowie et
62 al. (2006) observed that discrepancies between results obtained in different laboratories during the
63 IRONAGES comparison remained too large (e.g. up to 59% variability when using the same procedure)
64 and differed significantly at the 95 % confidence level. Factors thought to explain these results included:
65 (1) variations in the efficiency of the extraction of iron from the matrix during pre-concentration
66 (resulting in different procedures measuring different fractions of iron), (2) errors in the quantification of
67 the analytical blank, (3) inaccuracies in the system calibration and (4) underestimation of the stated
68 uncertainty (Bowie et al, 2003; Petrov et al. 2007). Hence iron data from these exercises for the same
69 water mass were distinctly inconsistent. Points (1) and (2) have been addressed by the SAFe (Johnson et
70 al., 2007) and GEOTRACES (GEOTRACES, 2013) exercises but not points (3) and (4). It is thus useful to
71 revisit these two factors and determine how realistic uncertainties can be estimated for the most
72 commonly applied measurement procedures (particularly shipboard procedures) (see also Ussher et al.,
73 2010b). In this respect flow injection with chemiluminescence detection (FI-CL) was chosen for this study
74 as it is a technique that allows high temporal and spatial resolution measurements at sea without the
75 need for sample storage and transport.

76 According to the international nomenclature, the measurement uncertainty is a "*non-negative parameter*
77 *characterizing the dispersion of the quantity values being attributed to a measurand, based on the*
78 *information used*" (JCGM 200, 2008). The basic purpose of an uncertainty statement is to propose a

79 range of possible 'true' values. There are various ways of estimating uncertainties. For instance,
80 combined uncertainty estimates can be based on data obtained by inter-laboratory or intra-laboratory
81 studies (see e.g. Analytical Methods Committee, 1995; Nordic Committee on Food Analysis, 1997). The
82 uncertainty estimation proposed in the Guide for Uncertainty in Measurements (GUM) is based on
83 combining the contributions of all known sources of uncertainty (JCGM 100, 2008). In this approach, the
84 measurement procedure is described by a mathematical model and the values and associated standard
85 uncertainties of the different components (the input quantities) in the model must be established. The
86 model and input data are then used to calculate the measurement result including its associated
87 combined uncertainty.

88 The aim of this work was to study the application of the 'GUM approach' to the FI-CL measurement
89 procedure. The specific objectives were to; (1) propose a set of mathematical equations (a model)
90 describing this measurement process and allowing the estimation of a measurement uncertainty, (2)
91 discuss the best way to assess the uncertainties of the different components in the model, (3) apply this
92 uncertainty model to present the measurement results with their estimated combined uncertainties
93 obtained for seawater samples from the SAFe and GEOTRACES campaigns (Lohan et al., 2006; Johnson
94 et al., 2007) and, from the above, (4) propose a simplified equation to estimate the measurement
95 uncertainty.

96

97 **Materials and procedures**

98 ***Reagents, materials and samples***

99 Concentrated hydrochloric acid (HCl), ammonia (NH₃, 20 – 22%) and glacial acetic acid (CH₃CO₂H), all
100 SpA grade, were purchased from Romil (Cambridge, UK). Hydrogen peroxide, Merck Suprapur grade was
101 obtained from VWR (Lutterworth UK). Luminol (5-amino-2,3-dihydro-1,4-phthalazinedione), sodium
102 carbonate and triethylenetetramine (TETA) were purchased from Sigma Aldrich (Gillingham, Dorset, UK).
103 All high purity water (HPW), 18.2 MΩ·cm, was drawn from an ElgaStat Maxima system (Marlow, UK). All
104 weighing was performed using an analytical balance (OH1602/C, Ohaus, Thetford, UK). The accuracy of
105 the balance was checked daily before use using F1 Class certified weights (KERN, Albstadt, Germany). All
106 facilities were managed under ISO 9001:2008 certification.

107 To ensure low blank Fe amount content all sample and reagent handling was undertaken in an ISO
108 14644-1 Class 5 laminar flow hood (Bassaire, Southampton, UK) situated within an ISO 14644-1 Class 5
109 clean room. Reagent and sample containers were made of low density polyethylene (LDPE; Nalgene,
110 Fisher Scientific, UK) and were cleaned using established cleaning protocols for trace metals. Containers
111 were immersed in ~ 1.1 M trace metal grade HCl (Fisher Scientific) for at least seven days. Subsequently,

112 the containers were rinsed in copious amounts of HPW, filled with 0.01 M HCl and stored in double re-
113 sealable plastic bags until use.

114 The main characteristics of the seawater samples used for this project are described in Table 1. Briefly,
115 all samples were filtered at sea and then acidified either at sea or at Plymouth University (PU). Seawater
116 samples, referred to as SWA, SWB, and SWC, containing $\leq 0.5 \text{ nmol kg}^{-1}$ Fe were selected to prepare
117 three different sets of calibration standards, by addition of controlled amounts of iron from a CPI
118 International (Amsterdam, Netherlands) ICP-MS standard containing 0.17 mol kg^{-1} Fe. Experiments in this
119 work were carried out with 0.5 L reference samples from large volumes of homogenised, bulk seawater
120 samples (SAFe D2 and GEOTRACES GS and GD consensus mean reference materials). More details
121 regarding the sampling, pre-treatment and bottling procedures for these materials can be found
122 elsewhere (Jonhson et al., 2007; GEOTRACES 2013).

123

124 ***The FI-CL based measurement procedure***

125 Figure 1 describes the FI-CL manifold used for these experiments. It consists of three peristaltic pumps
126 (Minipuls 3, Gilson, Luton, UK), one PTFE manually operated three port valve (Valve 1; Omnifit), one
127 three port solenoid valve (Valve 2), one two-way six port electronically actuated valve (Valve 3; VICI,
128 Valco Instruments, Schenkon, Switzerland), a thermostatic water bath (Gran, Cambridge, UK) and a
129 photomultiplier tube (PMT; Hamamatsu H 6240-01, Hamamatsu Photonics, Welwyn Garden City, UK)
130 containing a coiled, transparent PVC flow cell (volume $40 \mu\text{L}$). The peristaltic pump tubing used was two
131 stop accu-rated™ PVC (Elkay, Basingstoke, UK) and all other manifold tubing was 0.8 mm i.d. PTFE. The
132 system used two poly(methyl methacrylate) columns (1 cm long, 1.5 mm i.d., volume $70 \mu\text{L}$), loaded with
133 Toyopearl AF Chelate 650 resin (Tosoh Bioscience, Stuttgart, Germany) retained with HDPE frits (BioVion
134 F, 0.75 mm thick, 22-57 μm pore size), to clean up the buffer and column rinse solutions. The analytical
135 column, also loaded with Toyopearl AF Chelate 650 resin, was made of polyethylene with LDPE frits with
136 an internal volume of $200 \mu\text{L}$ (Global FIA, Fox Island, USA).

137 Peristaltic pump and valve control and data acquisition were performed using custom built hardware and
138 software (Ruthern Instruments, Bodmin, UK) run under Labview v 7.1 (National Instruments, Newbury,
139 UK). The measurement procedure, based on Obata et al. (1993), was as follows. A working solution of
140 approximately $0.35 \mu\text{mol kg}^{-1}$ Fe was prepared gravimetrically by serial dilution of the CPI International
141 stock solution. This working solution was then used to gravimetrically prepare calibration standards and
142 achieve added levels ranging from 0.15 to 0.9 nmol kg^{-1} Fe in $0.15 \text{ nmol kg}^{-1}$ increments. All calibration
143 standards were prepared at least 12 h before use to allow for complete equilibration of the added Fe with
144 that present in the calibration seawater. A $20 \mu\text{L}$ aliquot of a 10 mM H_2O_2 solution was added to all
145 calibration standards at least 2 h before use, to ensure that all Fe present was as Fe(III) (Lohan et al.,
146 2006). The following solutions were also prepared at least 12 h before use. A 48 mM stock solution of

147 luminol was obtained by dissolving 0.177 g of luminol and 0.25 g of Na_2CO_3 in 20 mL of HPW. This stock
148 was then diluted to give a 0.24 mM working solution. The post column reagents for the
149 chemiluminescence reaction was a mixture of 0.23 M HCl, 0.44 M NH_3 , 0.24 mM luminol / 0.46 mM TETA
150 and 0.31 M H_2O_2 . The acidified reference samples and standards of seawater were buffered to pH 3.5
151 with 0.35 M $\text{CH}_3\text{CO}_2\text{H}$ and 0.11 M NH_3 . To precondition and wash the column, 0.011 M HCl was used.
152 To operate the FI-CL instrument, the LabVIEW software was opened and the baseline signal from the
153 PMT monitored to check for stability. The pump controlling the eluent and post-column reagents was
154 then activated and the baseline chemiluminescence signal recorded after the signal had stabilised. Each
155 analytical session started with the measurement of a procedural blank (by application of the "closed
156 sample valve" method). For this, the sample flow was stopped, by closing one port on valve 1, so that
157 only the wash solution and ammonium acetate buffer passed over the column. The FI-CL system was
158 then operated by loading and injecting SWA for at least 30 min to monitor stability. Subsequently,
159 calibration seawater standards and samples were analysed. The FI-CL manifold was fully automated and
160 one replicate measurement consisted of the following analytical cycle. The column was conditioned for 10
161 s with 0.011 M HCl. Then the sample and buffer were loaded simultaneously for 60 s. The column was
162 washed with 0.011 M HCl for 20 s. The Fe was then eluted with 0.23 M HCl for 120 s. The mass of loaded
163 sample or standard solution was gravimetrically determined for each replicate by differential weighing.
164 Between each sample the sample flow path was washed with HPW for 30 s followed by uptake of the
165 fresh sample for 180 s. After each analytical session all fluid paths were flushed with 0.01 M HCl for 10
166 min and then with HPW for 15 min and HPW was left in the lines.

167

168 ***Data treatment***

169 Data integration was also performed with the custom build software run in LabVIEW. The baseline, and
170 the start and end points of the peak were set manually for each transient signal. The main calculations in
171 this study were carried out on the basis of peak height data, as this is the commonly used practice for FI-
172 CL measurements in the oceanographic community (and the wider FI community). Peak area
173 measurements were also made and some of the differences observed when using peak areas are
174 discussed below. Further data treatment, including calculations for the estimation of standard
175 uncertainties, was carried out in Excel[®]. The combined uncertainties were obtained by propagating
176 together individual uncertainty components according to the GUM (JCGM 100, 2008). In practice, a
177 dedicated software program was used (Metrodata GmbH, 2003). The reported combined uncertainties
178 are expanded uncertainties and reported as $U = k u_c$ where u_c is the combined standard uncertainty and k
179 is a coverage factor equal to 2. If "the probability distribution characterized by y and $u_c(y)$ is
180 approximately normal and the effective degrees of freedom of $u_c(y)$ is of significant size" ("greater than

181 10'), "taking $k=2$ produces an interval having a level of confidence of approximately 95 %" (JCGM 100,
182 2008).

183

184 **Assessment**

185 ***Definition of the measurand***

186 The GUM states that a measurement begins with an appropriate specification of the measurand, the
187 particular quantity intended to be measured (JCGM 100, 2008). Iron exists in different physico-chemical
188 forms in seawater. Traditionally, filtration is performed to differentiate between the different physical size
189 fractions (Ussher et al., 2004, 2010a, Wu et al., 2001). Additionally, iron occurs in two oxidation states;
190 Fe(II) and Fe(III). Generally, Fe(III) predominates in oxygenated waters, of which most (80–99%) is
191 strongly complexed by organic ligands (Achterberg et al., 2001; Mawji et al., 2008; Gledhill and Buck,
192 2012). In this study the measurand is the amount content of Fe present in $<0.2 \mu\text{m}$ filtered and acidified
193 samples and is regarded as the dissolved fraction of the Fe present in the seawaters. The aim was to
194 obtain the Fe amount content in specific samples and therefore the uncertainties associated with the
195 sampling process and/or the sample conditioning phase have not been considered.

196

197 ***Experimental design***

198 Three different types of experiment were performed. Firstly, the stability of the analytical procedure was
199 checked with 5 measurements (6 replicates of each) performed over a period of 32 h for SWC (with and
200 without H_2O_2 addition) and a procedural blank (this was termed the "stability experiment"). Secondly, the
201 effect of small variations in the matrix was investigated by comparing the sensitivity achieved for the
202 three different seawaters (Table 1). On the first day, SWA was compared with SWB while on the second
203 day SWA was compared with SWC ("matrix experiment"). Thirdly, the FI-CL based procedure was applied
204 to the determination of iron in samples of three filtered and acidified seawater reference materials using
205 SWA for calibration ("sample experiment").

206

207 ***Calculating the dissolved Fe amount content in the samples and mathematical description of*** 208 ***the measurement procedure***

209 Implicit in the GUM "is the assumption that a measurement can be modelled mathematically to the
210 degree imposed by the required accuracy of the measurement" (JCGM 100, 2008). A measurand Y is
211 determined from various input quantities X_i through a functional relationship. These input quantities "may
212 themselves be viewed as measurands and may themselves depend on other quantities, including
213 corrections and correction factors" "that can contribute a significant component of uncertainty to the
214 result of the measurement" (JCGM 100, 2008). A mathematical description of the FI-CL measurement
215 procedure is given through equations 1 to 5 described in Table 2. The main equation in this procedure is

216 the calculation of the dissolved Fe amount content in a sample by dividing the blank corrected sample
217 intensity by the sensitivity of the system (Equation 1 in Table 2). The way the equations controlling these
218 three input parameters were established is discussed below.

219

220 Mass normalisation of the measurement signal

221 In most flow analysis methods incorporating a pre-concentration column, the amount of sample loaded is
222 assumed to remain the same for constant loading times and the resulting peak height signals (expressed
223 in V) are used for the calculations. Variations in the loaded mass are thus not corrected for. However, this
224 was found to be an issue as variations in sample mass were observed to be significant during the
225 "stability experiment", with about 5% decrease in the sample loaded from the first to the last
226 measurement (data not shown). During the "sample experiment" the average loaded mass for samples
227 was lower than for the standards, probably due to the fact that the samples were all run at the end of
228 the sequence and were therefore more likely to be affected by wear on the pump tubing, increased back
229 pressure on the analytical column and / or changes in the relative flow rates of the sample and buffer
230 lines (Figure 2). These results show the importance of weighing the amount of seawater loaded each
231 time and of normalising the peak signal (symbol I, in V) to the loaded mass (in kg). In addition,
232 gravimetric measurement, coupled with calibration of the analytical balance, provides tighter traceability
233 to SI (the kg) of the amounts of loaded samples than loading by volumetric means.

234 As a result of this finding, mass normalised signals (symbol J, in $V\ kg^{-1}$) were used throughout this study
235 for the calculations (Equation 2b, Table 2). Following the example given in Quétel et al. (2001), in
236 equations 2a, 3a and 4a unity multiplicative factors were introduced to carry standard uncertainties
237 associated with signal stability, data integration and matrix effects. Since these unity factors do not
238 influence the final results, but enable the propagation of sources of uncertainty, they are discussed in
239 more detail below.

240

241 Blank corrections

242 Assessment of overall blank levels that reflect the reality of sample contamination during the
243 measurement procedure is necessary. In the international inter-laboratory comparison exercise
244 IRONAGES, blanks were reported to range between 6 and 290% of the Fe content in the seawater
245 sample (Petrov et al., 2007). Moreover, participants had diverse ways of defining and assessing their
246 blanks (Bowie et al., 2006) and were, therefore, possibly overlooking different aspects of the
247 contamination process. Sources of contamination during FI-CL measurements include the Fe present in
248 reagents (i.e. the added H_2O_2 , the buffer and wash solutions and the chemiluminescence reagents) and
249 Fe leaching from laboratory ware and parts of the experimental set-up. Sample manipulations could also
250 be a major contributor to the analytical blank as was shown to be the case by Petrov et al. (2007) during

251 isotope dilution inductively coupled plasma mass spectrometry measurements using co-precipitation with
252 magnesium hydroxide for sample preparation. The Fe from the reagents of the chemiluminescence
253 reaction is normally included in the baseline. Baseline subtraction for the determination of net peak
254 height or peak area signals should therefore remove this possible bias. The influence of additions of
255 chemical reagents for the purpose of preserving and/or conditioning the samples (e.g. acid, H₂O₂) can be
256 assessed using double spiking of the reagents. Previous studies using FI-CL have shown their contribution
257 to be low / negligible if care is taken to select high purity reagents (Bowie et al., 2003; Bowie et al.,
258 2004; Klunder et al. 2010).

259 Descriptions of what a blank may represent are available from the International Union of Pure and
260 Applied Chemistry (IUPAC). A "procedural blank" is "*where the analytical procedure is executed in all*
261 *respects apart from the addition of the test portion*" (McNaught and Wilkinson, 1997; Inczedy et al.,
262 1998). Alternative measurement procedures for blank determination, such as the field blank approach or
263 varying sample loading times and extrapolating back to time zero (Bowie et al. 2004), were not suitable
264 as the former requires a matrix containing no analyte and the latter only accounts for reagents that are
265 loaded for a constant time e.g. the wash solution, but not those for which the amount loaded is variable
266 e.g. the pH adjustment solution.

267 In FI-CL, the signal obtained with the "closed sample valve" method as described above, i.e. loading only
268 buffer (Bowie et al., 2004; Ussher et al., 2010a), can be considered as a procedural blank. This method
269 was applied as no better alternatives could be found for estimating the level of contamination. The risk
270 that matrix effects and pH changes could influence final results due to fluctuations in the blank values
271 determined in this way is discussed below. Normalised signal intensities were calculated by division by
272 the average loaded sample mass (equation 3b). These blank values were 50-100 times lower than the
273 signals for the seawater samples. Unity multiplicative correction factors were used to propagate
274 uncertainties on stability and matrix effects (equation 3a) and are discussed in more detail below.

275

276 Calculation of the calibration slope

277 The FI-CL method has a different sensitivity for seawater than for ultra-pure water because of matrix
278 related effects (Bucciarelli et al., 2001). Thus, a common approach for the calibration under matrix-
279 matching conditions is to use a low level Fe seawater and fortify it with increasing amounts of Fe
280 (Bucciarelli et al., 2001; Bowie et al., 2004; Ussher et al., 2010a; Klunder et al., 2011). In this work, in
281 addition to the low level seawater alone (termed the 'zero' standard), six calibration standards were
282 prepared with Fe amount content ranging from 0.15 to 0.9 nmol kg⁻¹. Since measurements were
283 repeated 6 times for each calibration point, a total of 7 x 6 = 42 results were obtained. A linear
284 regression was plotted, with the masses of Fe loaded (in kg, obtained by multiplication of the standard Fe
285 mass fraction by the loaded mass of the replicate) on the x axis and the corresponding measured signal

286 intensities (in V) on the y axis. The 'behaviour' of the data was nearly the same irrespective of the scale
287 of observation, with replicate results spread randomly around the regression graph in more or less the
288 same way for all 6 standards prepared and tested. Common practice is to produce 3-4 replicates per Fe
289 level and work with average values. Thus, a more practical way of establishing the calibration curve
290 consists of plotting a linear regression between the group of 6+1 Fe amount content (C, in nmol kg⁻¹) on
291 the x axis and the corresponding average normalized intensities (J, in V kg⁻¹) on the y axis. The sensitivity
292 coefficient (F, in V nmol⁻¹), i.e. the slope, is obtained using equation 4b from Table 2 (see Figure 3).
293 Weighted regression can also be performed but the calculations are more complex. In a weighted
294 regression the higher the uncertainty on a y value the smaller the contribution of the y value to the
295 regression slope. This is especially important if the increase of values on the x axis can be related to an
296 increase of the standard uncertainty on corresponding values on the y axis. There was no difference with
297 this dataset at the 95% confidence level between weighted and unweighted regressions. This is probably
298 because the increase in the standard uncertainty with increased normalised intensity is limited. The
299 comparison between these two approaches is further discussed in the next section.

300

301 ***Assessing the standard uncertainties***

302 Individual uncertainty components and the factors influencing their standard uncertainties were
303 evaluated. This is necessary to enable a combined uncertainty estimation of the Fe amount content
304 results.

305

306 Uncertainty on mass normalised measurement signals

307 During the "sample experiment", the repeatability (short term signal stability) of mass-normalised
308 intensities (peak height based signals) for one measurement varied between 1.9 and 4.0% RSD (relative
309 standard deviation, n=6) while for the "stability experiment" repeatabilities varied between 2.4 and 4.9
310 %. These variations in RSD cannot be explained by variations in the specific characteristics of the sample
311 replicates since the same solution was measured throughout the "stability experiment". Moreover, as
312 illustrated in Figure 4, there was also a longer term variability component involved (within-sequence-
313 stability), and thus two sources of instability influencing the intensity values. Over the 32 h long analytical
314 sequence there was no clear trend, and as a result correction for drift was not possible. Therefore, the
315 approach proposed is to estimate typical values for both components from the outcome of an ANOVA
316 analysis and multiply the sample average mass normalised intensities by unity correction factors carrying
317 the uncertainty for these two components (δ_{rep_s} and δ_{stab_s}). Repeated intensity values per sample and
318 average intensity values from replicate samples were approximately normally distributed. The intensity
319 repeatability and the within-sequence-stability, determined using data from the "stability experiment",
320 were 4.1% and 6.3% respectively. Assuming independence between the intensity values used to

321 calculate both types of standard deviation, uncertainty estimations were carried out using these standard
 322 deviations divided by square root 6, i.e. the number of replicates and square root 5, i.e. the number of
 323 repeat measurements analysed in each case, to give values of 1.7% and 2.8% respectively.

324 Sample loading and standard preparation cannot be performed gravimetrically on board ship and
 325 therefore this is done volumetrically, which may cause additional sources of uncertainty. In this case, the
 326 set of equations described in Table 2 will change slightly and result in equation 6 as described below:

$$327 \quad C_S = \frac{\bar{I}_{R-S} \cdot \delta_{rep-S} \cdot \delta_{stab-S} \cdot \delta_{WtoV-S} - \bar{I}_{R-B} \cdot \delta_{stab-B} \cdot \delta_{rep-B} \cdot \delta_{matrix-B}}{F_{reg} \cdot \delta_{matrix-std}} \quad \text{equation 6}$$

328 As a consequence of not using mass normalization, the sensitivity factor is determined by regression of
 329 the intensity (expressed in V) with the concentration (nmol L⁻¹) and has the units V/nmol L⁻¹. Secondly,
 330 an extra unity multiplicative correction factor (δ_{WtoV-S}) was introduced to take account of the difference in
 331 the mass loading between samples and standards (Figure 2). Using this data set and assuming constant
 332 loading (i.e. without mass normalisation) its contribution to the final uncertainty budget was a few
 333 percent. Lastly, although the same approach can be used to quantify the uncertainty on the unity
 334 multiplicative factors of the intensity repeatability and within-sequence-stability, the values will be higher
 335 than in the case of mass normalization. It must be noted that the within-sequence-stability during on-
 336 board measurements might be different than in controlled laboratory conditions, but a specific
 337 assessment was not possible within the time frame of this study.

338 Uncertainty on blank corrections

339 The evaluation of the uncertainty on blank measurement signals was approached in a similar way as for
 340 the sample measurement signals. ANOVA analysis of the "stability experiment" results indicated 6.9%
 341 and 10% respectively for the intensity repeatability (n=5) and the within-sequence-stability. A unity
 342 multiplicative factor $\delta_{matrix-B}$ with a value of 1±0.2 was conservatively applied in equation 3a to account
 343 for the matrix differences between the blank samples and the standards used for calibration purposes.
 344 However, since the signal intensity for the analytical blank was about 50-100 lower than the intensity for
 345 the seawater samples in this project, this source of uncertainty on the blank correction had no influence
 346 on the combined uncertainties estimated for the Fe amount content in the samples investigated.

347

348 Uncertainty on the calibration slope

349 As discussed above, there are different statistical approaches that can be used to calculate the slope of
 350 the regression line (Miller, 1991; Press et al., 2012). Values obtained using different regression
 351 approaches are not significantly different at the 95% confident interval, but associated standard

352 uncertainties do vary (Table 3). The standard uncertainty on the slope when using average normalised
353 intensity values is the same whether the regression is weighted or unweighted. It is lower when using all
354 individual data in the unweighted regression because there are more data points that follow a normal
355 distribution. The importance of the number of standards and replicates on the size of the estimated
356 standard uncertainty of the slope was studied. In Table 4 it can be seen that the number of standards
357 used is a more important criterion than the number of replicates, but nevertheless the uncertainty on the
358 sensitivity factor also improves using 6 rather than 3 replicates. Small matrix differences between the
359 three seawaters tested in the "matrix experiment" did not lead to significant differences between the
360 slopes obtained for SWA, SWB and SWC. Therefore, no uncertainty factor for differences in the calibrant
361 matrix was applied.

362

363 **Discussion**

364 ***Application to seawater samples from the SAFe and GEOTRACES campaigns***

365 Since consensus values are available for the Fe amount content in samples from the SAFe and
366 GEOTRACES campaigns (GEOTRACES, 2013), these data were compared with results obtained by
367 application of the model for combined uncertainty estimation and the calculations described above.
368 Samples D2, GS and GD were analyzed using 6 replicates each time, the "closed sample valve" approach
369 for blank assessment and a least square regression calibration line with 7 levels (no Fe added + 6 levels
370 of added Fe) in SWA. This was the "sample experiment", and results obtained are reported in Table 5.
371 Estimated expanded (coverage factor $k=2$) relative combined uncertainties were around 12% on a peak
372 height basis, and around 10% on a peak area basis. Using this dataset, the combined uncertainty was
373 slightly higher using volumetric loading compared with gravimetric loading. For example, for sample GD
374 the combined expanded uncertainty increased from 12 to 13% for peak height integration. It can be seen
375 that both peak height and peak area based results are systematically lower than the consensus values.
376 Results obtained for GS and GD (peak height and peak area basis) and peak area results for D2 were in
377 agreement with consensus values within uncertainty statements. These conclusions were reached from
378 the observation that the expanded combined uncertainty ($k=2$) on the difference between a measured
379 and the corresponding consensus value was greater than the difference itself in all cases (calculations
380 according to a methodology reported in Linsinger, 2010). For the peak height results for the D2 sample,
381 the expanded uncertainty on the difference was smaller than the difference itself but only by less than
382 3%. These results validate the measurement procedure implemented and the uncertainty estimation
383 process developed. They nevertheless point to the presence of a systematic effect not yet (sufficiently)
384 corrected for.

385

386 An overview of the values of the input parameters and their associated standard uncertainties for these
 387 experiments is given in supplementary Table S1. The relative contributions of the different input
 388 parameters to the uncertainty budget are given for sample GD in Table 6 as an example. The normalised
 389 signal intensity repeatability accounts for only 7.9% of the total uncertainty. The within-sequence-stability
 390 (assessed over 32 h) and the uncertainty on the sensitivity coefficient (calibration slope) are the most
 391 important contributors to the combined uncertainty with relative contributions of 21.6 and 69.7%.
 392 Therefore, it is beneficial to have a low uncertainty on the calibration slope. For this reason, it is
 393 favourable to use sufficient replicates (6) and number of standards (at least the non-spiked standards
 394 and 5 spiked levels). Moreover, correctly estimating the within-sequence-stability is key and should be
 395 done under the same measurement conditions as for the samples.

396
 397 Results obtained indicate that an uncertainty estimation based on the signal repeatability alone, as is
 398 often done in FI-CL studies, is not a realistic estimation of the overall uncertainty of the procedure.
 399 However, taking into account only the major contributions, the combined expanded uncertainty could be
 400 approximated using equation 7:

401

$$402 \quad U_{C_s} \approx 2 \cdot C_s \sqrt{\frac{\bar{J}_S^2 \cdot \left[\left(\frac{u_{\delta_{rep_S}}}{\delta_{rep_S}} \right)^2 + \left(\frac{u_{\delta_{stab_S}}}{\delta_{stab_S}} \right)^2 \right]}{(\bar{J}_S - \bar{J}_B)^2} + \left(\frac{u_F}{F} \right)^2} \quad \text{equation 7}$$

403
 404 In this, the standard uncertainty on the intensity repeatability and within-sequence-stability can be
 405 assessed using ANOVA analyses of repeat measurements of the same solution. The uncertainty on the
 406 calibration slope can be obtained using statistical tools. This simplified approach assumes that the blank
 407 does not significantly contribute to the uncertainty and should therefore have a much lower intensity
 408 compared with the sample (as was the case in this study). When using data from this project the
 409 uncertainty obtained with equation 7 was nearly identical to the uncertainty calculated above (for
 410 example the difference was less than 0.2% for GD using peak height data). Therefore, if the assumptions
 411 are valid this simplified approach provides a realistic uncertainty estimate.

412
 413 ***Peak area versus peak height***

414 The bias between results and consensus values was around -12% for D2 and GS and -20% for GD, on a
 415 peak height basis, and around -8% for D2 and GS and -16% for GD, on a peak area basis. This also
 416 means that peak height results were systematically lower than the peak area results by approximately 4-

417 5%. The cause for this trend is not well understood. It is unlikely to be related to an error in the
418 placement of the baseline for integration, as this affects height less than area (Dyson et al., 1998). In
419 contrast, the asymmetry of the FI-CL peaks could be a possible source of error during peak height
420 measurement, since peak area is less sensitive to peak asymmetry than peak height (Dyson et al., 1998).
421 It can also be observed in Table 5 that estimated combined uncertainties are larger for peak height than
422 for peak area based results. This is mainly related to a larger uncertainty associated with the sensitivity
423 coefficient for peak height compared with peak area (Table S1). The intensity repeatability and the
424 within-sequence-stability are also slightly better for peak area than for peak height data, which can be
425 related to count statistics. Area integration is considered the 'true' measure of the amount of solute
426 (Dyson et al., 1998) and possible problems specific to peak area data such as peak overlap and / or low
427 S/N ratios (Dyson et al., 1998) are not an issue with FI-CL measurements. These observations lead to the
428 conclusion that peak area data may be preferable to peak height data with FI-CL measurement results,
429 contrary to common practice. Additionally, users should routinely and systematically describe the way
430 peak data are processed.

431

432 **Comments and recommendations**

433 The amount content of dissolved Fe in marine waters is measured to elucidate the biogeochemical cycling
434 of this element and its role in the oceanic sequestration of atmospheric CO₂. However, quantifying the
435 amount of Fe present in <0.2 µm filtered and acidified seawater samples remains a difficult analytical
436 task, and achieving reliable results is a challenging objective. Moreover, the uncertainty as part of the
437 measurement results is easily underestimated.

438 FI-CL is a technique commonly applied because of its portability and hence suitability for shipboard
439 deployment. This paper proposes that the relative expanded ($k=2$) combined uncertainty of the
440 measurement results using FI-CL in the described configuration cannot be better than about 10 to 15%
441 for seawater samples containing 0.5 to 1 nmol kg⁻¹ of dissolved Fe. When applied on-board ship the
442 minimum achievable uncertainty is likely to be even larger owing to the more challenging working
443 conditions compared with shore-based laboratories. Moreover, this paper emphasises the fact that it will
444 be beneficial to researchers to refine measurement practices in order to improve the likelihood of
445 achieving lower uncertainty targets. For FI-CL, the uncertainty associated with the calibration slope and
446 the within-sequence-stability are shown to be much greater sources of uncertainty than the intensity
447 repeatability alone. Experimental planning must therefore systematically address the identification of
448 strategies aimed at quantifying and minimising the role of these uncertainty contributors. These
449 strategies include the use of as many calibration standards as possible (ideally 5 plus the 'zero' standard
450 measured with 6 replicates) and measurements repeated regularly for the same sample over the entire
451 analytical sequence. It is also shown that more attention needs to be paid to the way FI-CL peak data are

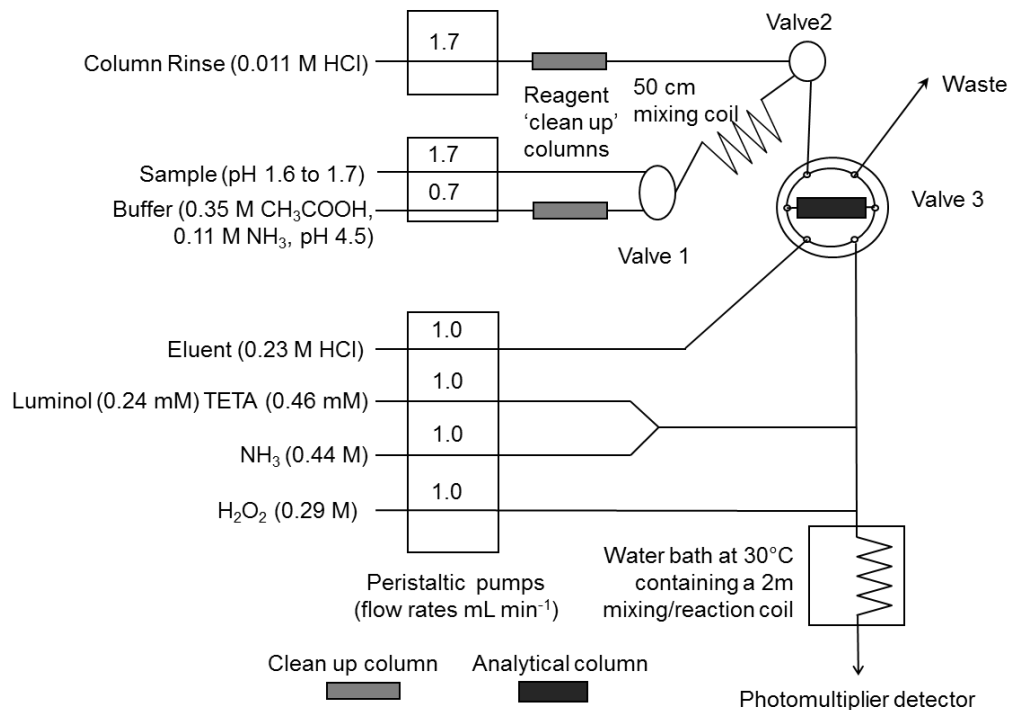
452 collected and processed, as this could lead to significant errors with respect to the size of the combined
453 uncertainties. To enhance the transparency of these aspects it is recommended that more comprehensive
454 descriptions of the methods used to validate the measurement procedures (including the way peak data
455 collection/processing is performed) are included in publications and reports. Moreover, a simple equation
456 to approximately estimate the uncertainty has been proposed, which is valid if the blank levels are
457 significantly lower than the levels of interest.

458 **References**

- 459 • Achterberg, E.P., T.W. Holland, A.R. Bowie, R.F.C. Mantoura and P.J. Worsfold, 2001.
460 Determination of iron in seawater. *Analytica Chimica Acta*, 442: 1-14.
- 461 • Analytical Methods Committee, 1995. Uncertainty of measurement: implications of its use in
462 analytical science. *Analyst* 120: 2303-2308.
- 463 • Bowie, A.R., E.P. Achterberg, S. Blain, M. Boye, P.L. Croot, P.L., H.J.W. de Baar, P. Laan, G.
464 Sarthou and P.J. Worsfold, 2003. Shipboard analytical intercomparison of dissolved iron in
465 surface waters along a north–south transect of the Atlantic Ocean. *Marine Chemistry* 84: 19-34.
- 466 • Bowie, A.R., E.P. Achterberg, P.L. Croot, H.J.W. de Baar, P. Laan, P., J.W. Moffett, S. Ussher and
467 P.J. Worsfold, 2006. A community-wide intercomparison exercise for the determination of
468 dissolved iron in seawater. *Marine Chemistry* 98: 81-99.
- 469 • Bowie, A.R., P.N. Sedwick and P.J. Worsfold, 2004. Analytical intercomparison between flow
470 injection-chemiluminescence and flow injection-spectrophotometry for the determination of
471 picomolar concentrations of iron in seawater. *Limnology and Oceanography: Methods* 2: 42-54.
- 472 • Boyd, P.W. and M.J. Elwood, 2010. The biogeochemical cycle of iron in the ocean. *Nature*
473 *Geoscience* 3: 675-682.
- 474 • Bucciarelli, E., S. Blain and P. Tréguer, 2001. Iron and manganese in the wake of the Kerguelen
475 Islands (Southern Ocean). *Marine Chemistry* 73: 21-36.
- 476 • Dyson, N., 1998. Chapter 2: Errors in peak area measurement. In *Chromatographic Integration*
477 *Methods*. The Royal Society of Chemistry. pp. 35-88.
- 478 • GEOTRACES, 2013. Dissolved Iron – values in nmol/kg Consensus values (± 1 std. dev.) for SAFe
479 Reference Samples as of May 2013. [http://www.geotraces.org/science/intercalibration/322-](http://www.geotraces.org/science/intercalibration/322-standards-and-reference-materials)
480 [standards-and-reference-materials](http://www.geotraces.org/science/intercalibration/322-standards-and-reference-materials) (last accessed July 15, 2014)
- 481 • Gledhill, M.B, and K.N. Buck, 2012. The organic complexation of iron in the marine environment:
482 A review. *Frontiers in microbiology* 3: 1-17.
- 483 • Inczedy, J., T. Lengyel, A. Ure, A. Gelencsér and A. Hulanicki, 1998. *Compendium of analytical*
484 *nomenclature*. Blackwell Science Ltd., Oxford, UK.
- 485 • ISO/IEC, General requirements for the competence of testing and calibration laboratories,
486 ISO/IEC 17025:2005, International Organization for Standardization/International Electrotechnical
487 Commission, Geneva, 2005.
- 488 • JCGM 100, Evaluation of measurement data — Guide to the expression of uncertainty in
489 measurement; Joint Committee for Guides in Metrology (BIPM, IEC, IFCC, ISO, IUPAC, IUPAP,
490 OIML, ILAC), BIPM, www.bipm.org, Paris, 2008.

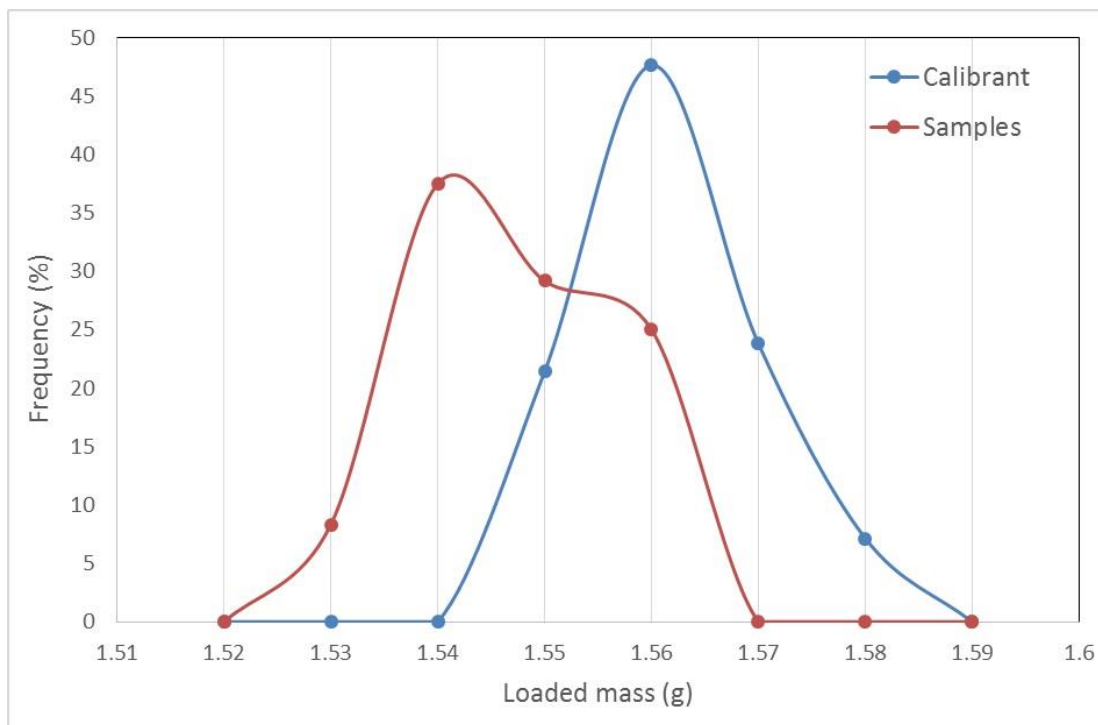
- 491 • JCGM 200, International vocabulary of metrology — Basic and general concepts and associated
492 terms (VIM); Joint Committee for Guides in Metrology (BIPM, IEC, IFCC, ISO, IUPAC, IUPAP,
493 OIML, ILAC), BIPM, www.bipm.org, Paris, 2008
- 494 • Johnson, K. S., E.Boyle, K. Bruland, K. Coale, C. Measures, J. Moffett, A. Aguilar-Islas, K.
495 Barbeau, B. Bergquist, A. Bowie, K. Buck, Y. Cai, Z. Chase, J. Cullen, T. Doi, V. Elrod, S.
496 Fitzwater, M. Gordon, A. King, P. Laan, L. Laglera-Baquer, W. Landing, Lohan, J. Mendez, A.
497 Milne, H. Obata, L. Ossiander, J. Plant, G. Sarthou, P. Sedwick, G. J. Smith, B. Sohst, S. Tanner,
498 S. Van den Berg and J. Wu, 2007. Developing standards for dissolved iron in seawater. *Eos*,
499 *Transactions of the American Geophysical Union* 88: 131-132.
- 500 • Klunder, M., P. Laan, R. Middag, H. de Baar and J. Van Ooijen, 2011. Dissolved iron in the
501 Southern Ocean (Atlantic sector). *Deep Sea Research Part II: Topical Studies in Oceanography*
502 58: 2678-2694.
- 503 • Linsinger, T., 2010. Comparison of a measurement result with the certified value. *European*
504 *Reference Materials: Application Note 1*.
- 505 • Lohan, M.C., A.M. Aguilar-Islas and K.W. Bruland, 2006. Direct determination of iron in acidified
506 (pH 1.7) seawater samples by flow injection analysis with catalytic spectrophotometric detection:
507 Application and intercomparison. *Limnology and Oceanography: Methods* 4: 164-171.
- 508 • Martin, J. and S. Fitzwater, 1988. Iron deficiency limits phytoplankton growth in the north-east
509 Pacific subarctic. *Nature* 331: 341-343.
- 510 • Mawji, E., M. Gledhill, J.A. Milton, G.A. Tarran, S. Ussher, A. Thompson, G.A. Wolff, P.J.
511 Worsfold, and E.P. Achterberg, 2008. Hydroxamate siderophores: Occurrence and importance in
512 the Atlantic Ocean. *Environmental Science & Technology* 42: 8675-8680.
- 513 • McNaught, A.D. and A. Wilkinson, 1997. *Compendium of chemical terminology*, Blackwell Science
514 Oxford.
- 515 • Metrodata GmbH, 2003. *Gum Workbench*. The software tool for the expression of uncertainty in
516 measurement. Metrodata GmbH, D-79639 Grenzach-Wyhlen, Germany.
- 517 • Miller, J.N., 1991. Basic statistical methods for analytical chemistry. Part 2. Calibration and
518 regression methods. A review. *Analyst* 116: 3-14.
- 519 • Mills, M.M., C. Ridame, M. Davey, J. La Roche and R.J. Geider, (2004) Iron and phosphorus co-
520 limit nitrogen fixation in the eastern tropical North Atlantic. *Nature* 429: 292-294.
- 521 • Nordic Committee on Food Analysis (NMKL), 1997. Pathogenic *Vibrio* species. Detection and
522 enumeration in foods. Method n°156 (UDC 576.851)
- 523 • Obata, H., H. Karatani and E. Nakayama, (1993) Automated determination of iron in seawater by
524 chelating resin concentration and chemiluminescence detection. *Analytical Chemistry* 65: 1524-
525 1528.

- 526 • Petrov, I., C.R. Quétel and P.D.P. Taylor, (2007) Investigation on sources of contamination, for
527 an accurate analytical blank estimation, during measurements of the Fe content in seawater by
528 isotope dilution inductively coupled plasma mass spectrometry. *Journal of Analytical Atomic*
529 *Spectrometry* 22, 608-615.
- 530 • Press, W.H., 2012. *Numerical Recipes in C: The Art of Scientific Computing*.
- 531 • Quétel, C.R., T. Prohaska, S.M. Nelms, J. Diemer and P.D.P. Taylor, 2001. ICP-MS applied to
532 isotope abundance ratio measurements: performance study and development of a method for
533 combining uncertainty contributions from measurement correction factors. In: G. Holland and S.
534 Tanner (Editors), *Plasma Source Mass Spectrometry: The New Millennium*. 7th Durham
535 Conference Royal Society of Chemistry, Cambridge, pp. 257
- 536 • Ussher, S.J., E.P. Achterberg, C. Powell, A.R. Baker, T.D. Jickells, R. Torres and P.J. Worsfold,
537 2013. Impact of atmospheric deposition on the contrasting iron biogeochemistry of the North and
538 South Atlantic Ocean. *Global Biogeochemical Cycles* 27: 1-12.
- 539 • Ussher, S.J., E.P. Achterberg, G. Sarthou, P. Laan, H.J.W. de Baar and P.J. Worsfold, 2010a.
540 Distribution of size fractionated dissolved iron in the Canary Basin. *Marine Environmental*
541 *Research* 70: 46-55.
- 542 • Ussher, S.J., E.P. Achterberg and P.J. Worsfold, 2004. Marine Biogeochemistry of Iron.
543 *Environmental Chemistry* 1: 67-80.
- 544 • Ussher, S.J., I. Petrov, C.R. Quétel and P.J. Worsfold, 2010b. Validation of a portable flow
545 injection–chemiluminescence (FI-CL) method for the determination of dissolved iron in Atlantic
546 open ocean and shelf waters by comparison with isotope dilution–inductively coupled plasma
547 mass spectrometry (ID-ICPMS). *Environmental Chemistry* 7: 139-145.
- 548 • Wu, J.F., E. Boyle, W. Sunda and L.S. Wen, 2001. Soluble and colloidal iron in the oligotrophic
549 North Atlantic and North Pacific. *Science* 293: 847-849.
- 550 • Wyatt, N.J., A. Milne, E.M.S. Woodward, A.P. Rees, T.J. Browning, H.A. Bouman, P.J. Worsfold
551 and M.C. Lohan, 2014. Biogeochemical cycling of dissolved zinc along the GEOTRACES South
552 Atlantic transect GA10 at 40°S. *Global Biogeochemical Cycles* 10.1002/2013GB004637.
- 553



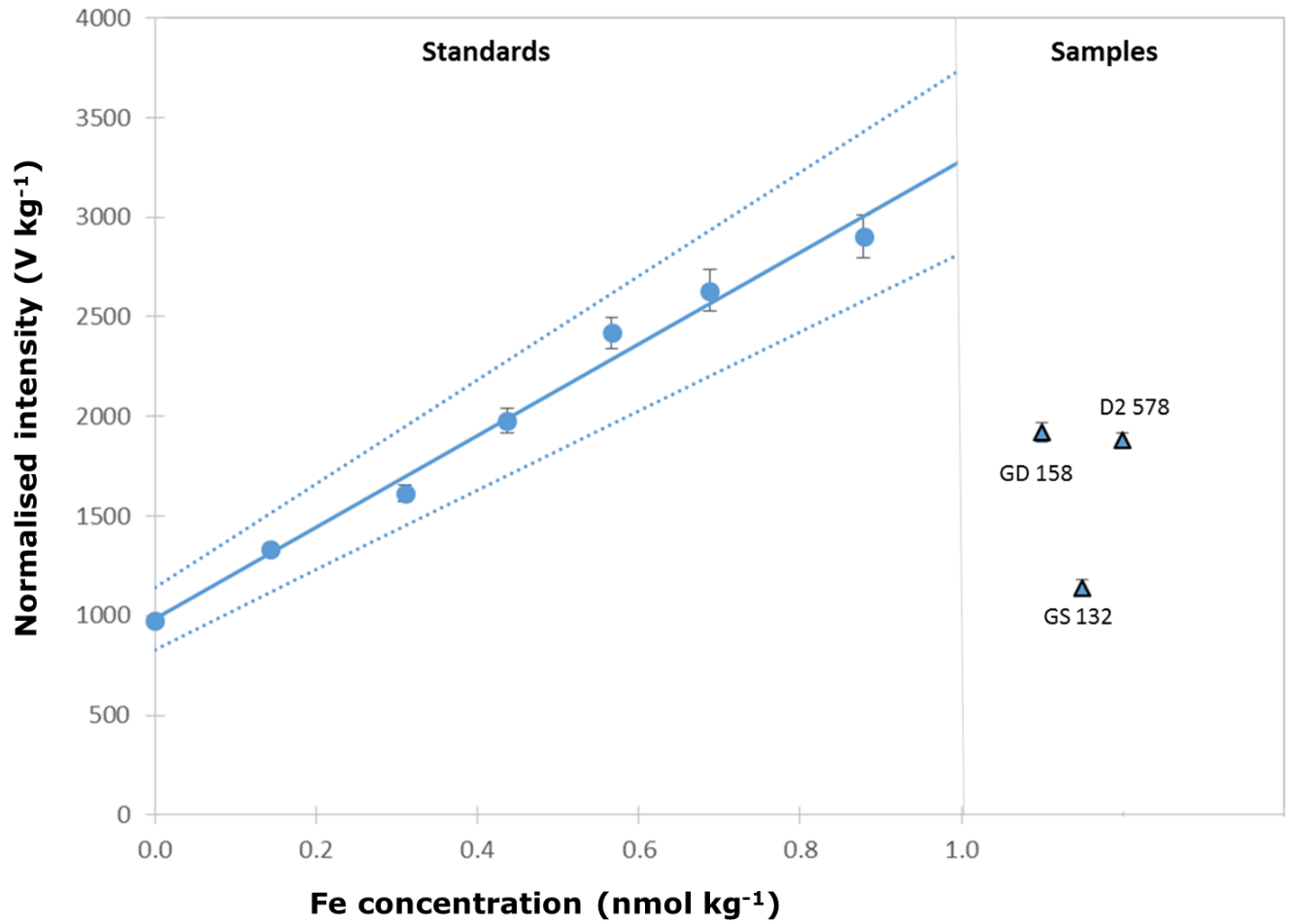
554
555
556

Figure 1: The FI-CL system used for the determination of dissolved Fe levels in seawater.

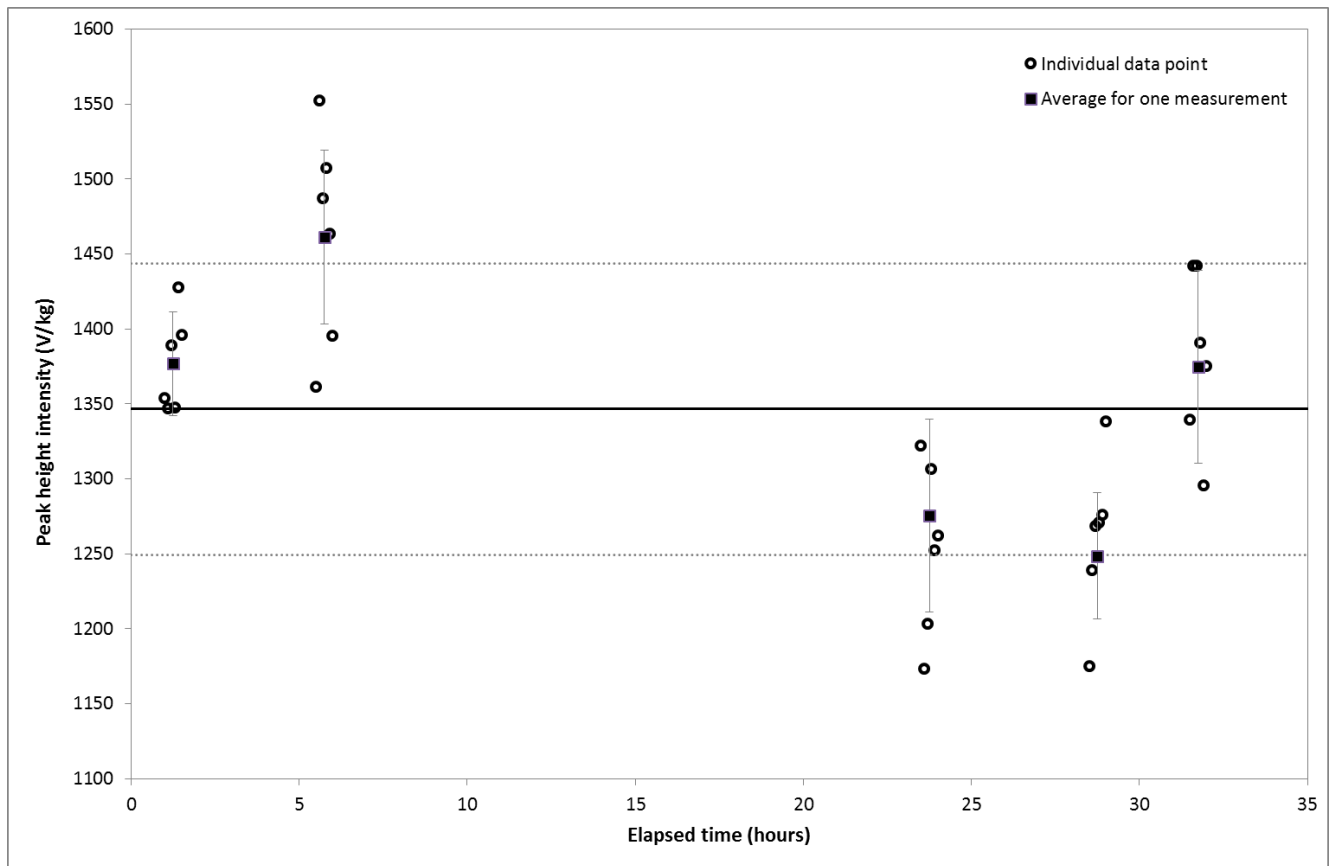


557
558
559
560

Figure 2: Frequency of variation (in %) of loaded masses for samples and calibration standards during the "sample experiment"



561
 562 Figure 3: Unweighted calibration using average data for the regression. Blue dotted lines delimit a 95%
 563 confidence interval around the regression graph. Signal intensities observed for samples GD158, GS132 and
 564 D2578 are also reported.
 565
 566
 567



568

Figure 4: Stability over the 32 h “stability experiment” with seawater C using peak height based results. Vertical bars indicate the standard deviation of the average of the 6 replicates. Horizontal lines indicate the average and standard deviations for the groups of 5 repeat measurements.

569

570 **Table 1: Description of the samples used.**

Sample name	SWA	SWB	SWC	SAFe campaign	GEOTRACES campaigns	
				D2-578	GS-132	GD-158
Collection Location	05°20.5' S, 06°11.9' W to 06°44.8' S, 05°04.8' W	27° 47.195' S, 007°12.949' W	40° S 48.46° W	30° N, 140° W	31°40' N 64°10' W	31°40' N 64°10' W
Depth	Surface	500 m	Surface	1000 m	Surface	2000 m
Filtration	Sartorius Sartobran-P cartridge. Cellulose acetate 0.45 µm pre-filter then 0.2 µm filter	Whatman GD/X PTFE 0.2 µm filter	Pall Acropak Supor capsule. PES 0.8 pre-filter then 0.2 µm filter.	Polycarbonate track etched 0.45 µm pre-filter, then 0.2-µm filter. Homogenized in 1000 L fluorinated LDPE tanks	Pall Acropak Supor capsule. PES0.8 pre-filter then 0.2 µm filter.	
Acidification	Bulk sample acidified at sea with 700 mL of ~10 M Q-HCl. Homogenized in 1000 L fluorinated LDPE tanks	Acidified at Plymouth University (PU) with 2 mL of Romil UpA grade HCl per L seawater	Acidified at PU with 1 mL of Romil UpA grade HCl per L seawater	Acidified at sea with 2 mL of conc HCl per L seawater.	Homogenized in 500 L fluorinated LDPE tanks. Acidified at sea with 2 mL of conc HCl.	
Final pH	2.0	2.0	1.7	1.8	1.8	1.8
Consensus dissolved Fe ± 2 s.d. (nmol kg ⁻¹)	0.53 ± 0.20	N/A	N/A	0.933 ± 0.046	0.546 ± 0.092	1.0 ± 0.2
Reference	Bowie et al., 2006	Ussher et al., 2013	Wyatt et al., 2014	Lohan et al., 2006	Johnson et al, 2007	

571

Table 2: Mathematical equations for quantification of the Fe amount content using gravimetric loading and FI-CL based procedure.

1. Amount content in the sample C_S	
Blank corrected sample signal intensity divided by the sensitivity (calibration slope) of the measurement procedure :	
$C_S = \frac{\bar{J}_S - \bar{J}_B}{F}$	
2. Normalised signal intensity for the sample \bar{J}_S	
a. Normalised signal intensity for the sample accounting for all sources of uncertainty:	
$\bar{J}_S = \bar{J}_{R_S} \cdot \delta_{rep_S} \cdot \delta_{stab_S}$	
b. Average normalised raw signal intensity for consecutive replicates: $\bar{J}_{R_S} = \frac{1}{n} \sum_i \frac{I_{S-i}}{m_{S-i}}$	
3. Normalised signal intensity for the analytical blank \bar{J}_B	
a. Normalised signal intensity for the analytical blank accounting for all sources of uncertainty: $\bar{J}_B = \bar{J}_{R_B} \cdot \delta_{stab_B} \cdot \delta_{rep_B} \cdot \delta_{matrix_B}$	
b. Average normalised raw signal intensity for consecutive replicates under closed sample valve conditions: $\bar{J}_{R_B} = \frac{1}{n} \sum_i \frac{I_{B-i}}{\bar{m}_S}$	
4. Calibration slope F	
a. Slope accounting for all sources of uncertainty: $F = F_{reg} \cdot \delta_{matrix_std}$	
b. Slope of least squares regression line of the normalised signal intensity versus the amount added Fe:	
$F_{reg} = \frac{r \sum C_{std_j} \cdot \bar{J}_{std_j} - \sum C_{std_j} \cdot \sum \bar{J}_{std_j}}{r \sum C_{std_j}^2 - (\sum C_{std_j})^2}$	
5. Amount content of the added Fe in the calibration standards	
a. Added Fe amount in the calibration standard: $C_{std_j} = \frac{m_{stock_j}}{(m_{stock_j} + m_{calSW_j})} \cdot C_{stock}$	
b. Amount in the stock solution: $C_{stock} = \frac{m_{mother_aliquot}}{m_{stock} + m_{mother_aliquot}} \cdot C_{mother}$	

Parameter		Index	
C	Fe amount content (nmol kg ⁻¹)	S	Sample
I	Signal intensity (V)	B	Blank
\bar{J}	Average mass normalised intensity (V kg ⁻¹)	R	Raw
		Std	Calibration Standard
F	Sensitivity coefficient (slope, V nmol ⁻¹)	stock	Intermediate Fe standard stock solution (prepared dilution of the mother solution)
n	Number of replicates	mother	Mother Fe standard solution (commercial standard)
r	Number of calibration standards	i	Index referring to the x th sample replicate
m & \bar{m}	Mass & average mass (kg)	j	Index referring to the x th standard
		Reg	Sensitivity coefficient (calibration slope) obtained by linear regression
		calSW	a 'low iron' seawater substrate used to produce the calibration curves
δ	Unity multiplicative correction factors carrying the relative uncertainty associated to the parameter considered	Stab	Accounts for the uncertainty arising from the intensity stability over an analytical sequence
		matrix	Accounts for the uncertainty arising from matrix effects on the sensitivity
		rep	Accounts for the uncertainty arising from the intensity repeatability
		WtoV	Accounts for the uncertainty related to the difference in loaded mass whether it is done by weighing of volumetrically

577 **Table 3: Slopes and their associated standard uncertainties depending on the regression calculations**
 578 **considered. r is the number of standards and n the number of replicates per standard.**

Regression approach		Data points	Sensitivity coefficient (=slope) (F)	
			Value	Uncertainty (k=1)
Weighted regression		7 (r)	2301	83
Unweighted regression	average values		2297	118
	all individual data	42 (r*n)	2297	56

579
 580 **Table 4: Dependence of the relative standard uncertainty (rsu) on the calculated slope/sensitivity coefficient,**
 581 **rsu (F), in %, on the number of replicates or calibration standards used.**

n	rsu (F), with n = number of replicates using 7 calibration standards (original + 6 Fe addition levels)	rsu (F), with n = number of calibration standards using 6 replicates for each standard
6	6.6	6.6
5	7.5	6.8
4	7.9	11.5
3	8.6	14.6

582
 583 **Table 5: Amount content results with combined expanded uncertainty with a coverage factor (k) of 2 (i.e. 95%**
 584 **confidence interval) for the three sea water samples from the SAFe and GEOTRACES campaigns using**
 585 **gravimetric loading. Consensus values were downloaded from the GEOTRACES.org website and are from May**
 586 **2013.**

Sample	Obtained Fe amount content (nmol kg ⁻¹)				Consensus Fe amount content (nmol kg ⁻¹)	
	Peak height		Peak area		Value	Relative uncertainty
	Value	Relative uncertainty	Value	Relative uncertainty		
D2	0.82 ± 0.10	12	0.861 ± 0.086	10	0.933 ± 0.046	4.9
GS	0.478 ± 0.060	12	0.500 ± 0.051	10	0.546 ± 0.092	16.8
GD	0.800 ± 0.099	12	0.836 ± 0.084	10	1.0 ± 0.2	20.0

587
 588
 589
 590
 591
 592
 593
 594

595 **Table 6: Relative contributions (%) to the combined uncertainty budget estimated for the dissolved Fe level**
 596 **measured by FI-CL in the GD sample from the GEOTRACES campaign (symbols as in Table 2). The intermediate**
 597 **result refers to the parameters used in equation 1 of Table 2, in which all associated uncertainties are included.**

Quantity		Gravimetric loading	
		Peak height	Peak area
\bar{J}_S (V/kg)	Intermediate result	29.5	44.4
	\bar{J}_{R_S} (treated as constant)	-	-
	δ_{rep_S}	7.9	9.4
	δ_{stab_S}	21.6	35.0
\bar{J}_B (V/kg)	Intermediate result	0.6	1.4
	I_B (treated as constant)	-	-
	\bar{m}_S	0.0	0.0
	δ_{rep_B}	0.0	0.6
	δ_{stab_B}	0.1	0.0
	δ_{matrix_B}	0.5	0.8
F (sensitivity coefficient or slope) (V/nanomol)	Intermediate result	69.7	54.3
	F_{reg}	69.7	54.3
	δ_{matrix_std}	0.0	0.0

598

599

600 **Supplementary information**

601 Table S1: details of the uncertainty budget associated to the result of the measurement by FI-CL (with gravimetric loading) of the dissolved Fe amount
 602 content in the D2 reference material from SAFe. Symbols as in Table 2.

603

Quantity			Peak height			Peak area		
			Value	Stand Unc (k=1)		Value	Stand Unc (k=1)	
				Absolute	%		Absolute	%
\bar{J}_S (V/kg)	Intermediate result	D2	1918	63	3.3	52179	1700	3.3
		GS	1140	37	3.3	30809	1000	3.3
		GD	1879	62	3.3	50711	1700	3.3
	\bar{J}_{R_S}	D2	1918	0	0	52179	0	0
		GS	1140	0	0	30809	0	0
		GD	1879	0	0	50711	0	0
	δ_{rep_S}		1	0.017	1.7	1	0.015	1.5
	δ_{stab_S}		1	0.028	2.8	1	0.029	2.9
	\bar{J}_B (V/kg)	Intermediate result	41.8	2.2	5.3	1115	190	17.0
I_B		0.0645	0	0	1.72	0	0.0	
\bar{m}_S		0.001542	0.000004	0.3	0.001542	0.000004	0.3	
δ_{rep_B}		1	0.069	6.9	1	0.17	17.0	
δ_{stab_B}		1	0.10	10	1	0	0	
δ_{matrix_B}		1	0.2	20	1	0.2	20	
Intermediate result		2297	118	5.1	59330	2190	3.7	
F (sensitivity coefficient or slope) (V/nanomol)	F_{reg}	2297	118	5.1	59330	2190	3.7	
	δ_{matrix_std}	1	0	0	1	0	0	

604